Correlation of microwave dielectric properties and normal vibration modes of $x\mathrm{Ba}(\mathrm{Mg}_{1/3}\mathrm{Ta}_{2/3})\mathrm{O}_3-(1-x)\mathrm{Ba}(\mathrm{Mg}_{1/3}\mathrm{Nb}_{2/3})\mathrm{O}_3$ ceramics: I. Raman spectroscopy

Chih-Ta Chia,[a] Yi-Chun Chen, and Hsiu-Fung Cheng
Department of Physics, National Taiwan Normal University, Taipei, Taiwan 116, Republic of China

I-Nan Lin
Materials Science Center, National Tsing-Hua University, Hsinchu, Taiwan 300, Republic of China

(Received 11 February 2003; accepted 11 June 2003)

Micro-Raman measurements of $x\mathrm{Ba}(\mathrm{Mg}_{1/3}\mathrm{Ta}_{2/3})\mathrm{O}_3-(1-x)\mathrm{Ba}(\mathrm{Mg}_{1/3}\mathrm{Nb}_{2/3})\mathrm{O}_3$ perovskite ceramics, with $x=0$, 0.25, 0.50, 0.75, and 1.0, were taken at room temperature. Raman results clearly show the 1:2 ordered structures of these compounds. Four A_{1g} and five E_g Raman modes were unambiguously assigned. The $\mathrm{A}_{1g}(\mathrm{O})$ phonon of the oxygen-octahedron stretch mode, which possesses the largest energy and width of all the observed Raman phonons, significantly influences the microwave dielectric properties of the materials. A higher vibration frequency of $\mathrm{A}_{1g}(\mathrm{O})$ mode results in a lower dielectric constant, and a wider width of the mode corresponds to a lower $Q\times f$ value. © *2003 American Institute of Physics.* [DOI: 10.1063/1.1597968]

I. INTRODUCTION

The $A(B'_{1/3}B''_{2/3})\mathrm{O}_3$ ceramics with 1:2 ordered perovskite structures, are known for their remarkable microwave dielectric properties. Their characteristics of low dielectric loss and high Q value in the microwave region have great potential for industrial applications, such as a dielectric resonator.[1–3] Recently, the correlation of B-site ordering with microwave properties in similar ceramics, as elucidated by the Raman method, has been a subject of considerable interest.[4–11] A strong relationship between the ordered structure and the remarkable microwave properties has been found.[6,12]

In this study,

$$x\mathrm{Ba}(\mathrm{Mg}_{1/3}\mathrm{Ta}_{2/3})\mathrm{O}_3-(1-x)\mathrm{Ba}(\mathrm{Mg}_{1/3}\mathrm{Nb}_{2/3})\mathrm{O}_3$$

[hereafter xBMT$-(1-x)$BMN] ceramic samples were prepared, and their phonon properties were examined by Raman spectroscopy. The effect of the substitution of the Nb atom by the Ta atom in xBMT$-(1-x)$BMN materials on the Raman-active phonons was investigated. The phonon modes were assigned, and the correlation of phonon vibrations with the microwave properties was found.

II. EXPERIMENTS

xBMT$-(1-x)$BMN perovskite ceramic samples, with $x=0$, 0.25, 0.50, 0.75, and 1.0, were prepared by the conventional mixed oxide process, in conjunction with a hot isostatic pressing (HIP) technique. These samples were first conventionally sintered at 1580 °C in air and then ''hipped'' in a 99.9% Ar atmosphere in a Mo chamber. The temperature of the hipping chamber was raised to 1300 °C at a pressure of 1500 kg/cm^2, at which temperature it was held for 1 h, before being reduced to room temperature with at a rate of 16 °C per min; the argon pressure was gradually reduced to 1000 kg/cm^2. The pressure was finally released at room temperature. The dielectric properties were measured by the TE_{011} resonant cavity method using an HP 8722 network analyzer, near 6 GHz.[13,14] Raman measurements were taken at room temperature, and the signals were recorded by a DILOR XY-800 triple-grating Raman spectrometer, equipped with a liquid-nitrogen-cooled CCD. The 10-mW output of the 514.5-nm line of an Ar^+ ion laser was used as the excitation source. The obtained Raman spectra exhibited a resolution approximately 0.5 cm^{-1}.

III. GROUP THEORY ANALYSIS

The 1:2 ordered-structure of $\mathrm{Ba}(\mathrm{Mg}_{1/3}\mathrm{Nb}_{2/3})\mathrm{O}_3$ or $\mathrm{Ba}(\mathrm{Mg}_{1/3}\mathrm{Ta}_{2/3})\mathrm{O}_3$ materials belongs to $P\bar{3}m1(\equiv D^3_{3d})$ space group,[15] and its unit cell has 15 atoms. Total normal vibration modes predicted by factor group analysis are $4\mathrm{A}_{1g}+\mathrm{A}_{2g}+5\mathrm{E}_g+2\mathrm{A}_{1u}+7\mathrm{A}_{2u}+9\mathrm{E}_u$, $4\mathrm{A}_{1g}+5\mathrm{E}_g$ are Raman active, and $7\mathrm{A}_{2u}+9\mathrm{E}_u$ are IR active. Based on the notation of Wychkoff site and factor group analysis, the specific vibration modes for each site symmetry are determined, and listed in Table I. Nine Raman active modes, $4\mathrm{A}_{1g}+5\mathrm{E}_g$, are related only to the motion of Ba and Ta (or Nb) atoms at the $2d$ site, and the motion of O atoms at the $6i$ site. The normal vibrations of the $A(B'_{1/3}B''_{2/3})\mathrm{O}_3$ 1:2 ordered structure were depicted by Tamura *et al.*[16]

The infrared active phonons, which are the polar phonons, can be used to calculate the dielectric constant in the infrared and far-IR ranges,[13,17] and thus to extrapolate the microwave dielectric properties of complex perovskite materials. However, assigning IR-active modes is difficult, since the resonant peaks are highly diffuse. Raman scattering is highly sensitive to the composition of materials, and the changes of phonon line shape caused by the different composition are very useful for assigning phonons. Therefore, the Raman spectroscopy provides important information that

[a]Electronic mail: chiact@phy.ntnu.edu.tw

TABLE I. The site symmetry analysis for the vibration modes of $Ba(Mg_{1/3}Ta_{2/3})O_3$ and $Ba(Mg_{1/3}Nb_{2/3})O_3$ perovskite 1:2 ordered structure

Atom	Site symmetry	Normal modes
2Ba	2*d*	$A_{1g}+A_{2u}+E_g+E_u$
Ba	1*b*	$A_{2u}+E_u$
Mg	1*a*	$A_{2u}+E_u$
Ta (or Nb)	2*d*	$A_{1g}+A_{2u}+E_g+E_u$
6O	6*i*	$2A_{1g}+A_{2g}+3E_g+A_{1u}+2A_{2u}+3E_u$
3O	3*f*	$A_{1u}+2A_{2u}+3E_u$
Total Normal Modes		$4A_{1g}(R)+A_{2g}(s)+5E_g(R)+2A_{1u}(s)+7A_{2u}(IR)+9E_u(IR)$

correlates the vibration characteristics of the materials with the microwave dielectric properties, even though the Raman phonons of the complex perovskite materials are mainly nonpolar.

IV. RESULTS AND DISCUSSION

A. Raman results and phonon assignment

The variations of Raman shift and the full width at half-maximum (FWHM) of xBMT$-(1-x)$BMN, caused by Ta substitution, are two important fingerprints in identifying the normal modes. The Ta concentration ratio x, strongly affects the Raman line shape of Ta (or Nb) vibration modes in xBMT$-(1-x)$BMN, and insignificantly alters the phonon modes that correspond to Ba and O atomic motion. The frequency of the phonon is approximately inversely proportional to the square root of the mass of the atoms involved. When Nb atoms are replaced by heavier Ta atoms, the frequencies of the normal modes that involve the motion of Nb or Ta atoms are expected to be significantly redshifted, whereas those vibrations that involve O or Ba atomic motion are expected to show relatively small changes or to be quasi-invariant.

The typical Raman spectra of BMN and BMT have four main peaks, as discussed in Refs. 4 and 18; they are assigned to normal vibration modes related to the localized 1:1 ordered structure,[4,19,20] although the long-range 1:2 order is preserved. The Raman spectra of the normal vibrations of localized 1:1 ordered and long-range 1:2 ordered structure consist of four key features: (i) the Raman phonon with the lowest energy near 105 cm^{-1} corresponds to F_{2g}(Ba) of the 1:1 ordered structure; (ii) two modes associated with the vibration of O atoms near 400 cm^{-1} are F_{2g}(O) and E_g(O) modes; (iii) the broad peak near 800 cm^{-1}, which corresponds to A_{1g}(O) of the 1:1 ordered structure is the stretch mode of the oxygen octahedron; (iv) three more weak phonons are also detected between 150 and 300 cm^{-1}, and they are strongly related to the long-range 1:2 ordered structure.[4] According to these four features, the obtained Raman spectra are depicted in Figs. 1(a)–1(d). Figure 1(a) depicts the phonon modes near 105 cm^{-1}, associated with F_{2g}(Ba) in 1:1 ordered structure, and Fig. 1(b) presents the phonons related to the 1:2 ordered structure. Figure 1(c) shows the phonons associated with the F_{2g}(O) and E_g(O) modes of 1:1 ordered structure, while Fig. 1(d) shows the oxygen-octahedron stretch A_{1g}(O) modes.

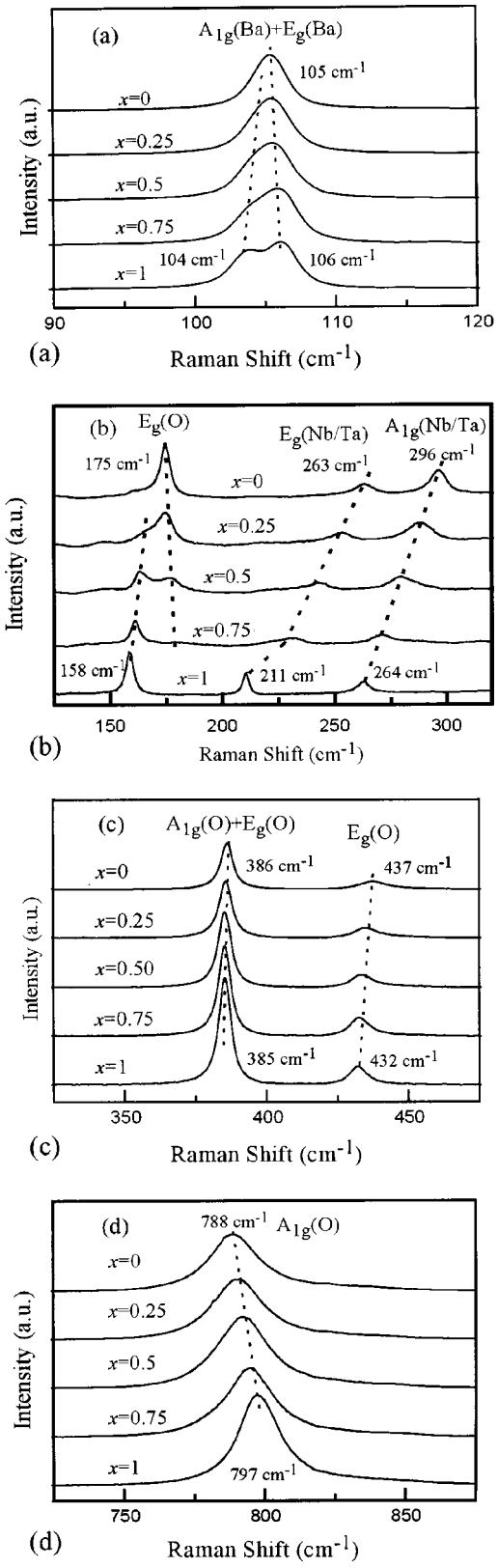

FIG. 1. The Raman spectra of xBMT$-(1-x)$BMN materials with $x=0$, 0.25, 0.5, 0.75, and 1. (a) Phonons related to the Ba atomic motion near 105 cm^{-1}; (b) the 1:2 ordered phonons; (c) modes related to the O atomic motion in between 350 and 450 cm^{-1} and (d) the oxygen-octahedron stretch modes.

According to the Raman measurements in Figs. 1(a)–1(c), most phonon modes are significantly redshifted and quasi-invariant, or slightly redshifted. The Ba vibration mode at 105 cm^{-1} and the O vibration modes near 386 and 437~432 cm^{-1} are relatively insensitive to the Ta concentration, as shown in Figs. 1(a) and 1(c). Notably, the 105-cm^{-1} vibration mode splits into two Raman peaks as the Ta concentration ratio x increases. Based on the analysis of the crystal symmetry, the localized 1:1 ordered F_{2g} mode is split into A_{1g} and E_g modes when the long-range 1:2 order is preserved. The splitting of F_{2g}(Ba) clearly found in the BMT sample indicates these two modes can be assigned to A_{1g}(Ba) and E_g(Ba). However, the splitting of F_{2g}(O) at 386 cm^{-1} is not observed for any sample, implying that the A_{1g}(O) and E_g(O) modes always overlap. We expect these two modes of the BMT can be resolved at a lower temperature. In Fig. 1(c), the peak near 437 cm^{-1}, whose vibration frequency decreases slightly but monotonically with x, corresponds to the E_g(O) mode.

Although phonon modes are expected to shift to lower frequencies, due to Ta, substitution, an exception exists. The phonon around 788~797 cm^{-1} shown in Fig. 1(d), corresponding to the A_{1g}(O) stretch mode, is the only one to be blueshifted as x increases. We think the large Ta atom increases the stiffness of the oxygen octahedral cage,[19,21] causing a blueshift for the stretch-vibration A_{1g}(O) mode. This mode is unambiguously identified as the oxygen-octahedral stretch mode.[4–6,17,19,20]

The two 1:2 long-range-ordered modes near 296~264 and 263~211 cm^{-1}, as shown in Fig. 1(b), are markedly redshifted, by 30 to 50 wave numbers as x varies from 0 to 1. These two vibration modes show similar variations of their line shapes as x increases. The profound influence of Ta substitution indicates that these two phonons are directly related to the normal modes that involve Ta or Nb atomic motion. The mode, that varies from 263 to 211 cm^{-1}, is the E_g(Ta/Nb) mode. The mode near 296~264 cm^{-1} is the A_{1g}(Ta/Nb), since the A_{1g} mode is expected to have a higher energy than the E_g mode.[4,19,22,23] The 1:2 ordered phonon near 175~158 cm^{-1}, which is also considerably influenced by the Ta substitution, cannot be the normal mode associate with the motion of Ta (or Nb) atoms. It splits into two peaks, instead of shifting when Ta and Nb coexist in the compounds. Similar phonon splitting behavior was found in the A_{1g}(O) stretch mode of BMN when Mg is at the Nb lattice site, and the ratio of the intensities of these two splitting peaks represents the degree of 1:2 order of the structure.[5] The mode near 175~158 cm^{-1} behaves like the BMN A_{1g}(O) stretch mode in Ref. 5. Therefore, it is the E_g(O) mode. Having identified the three weak signals of the 1:2 long-range-order phonons as associated with the E_g(O), E_g(Ta/Nb) and A_{1g}(Ta/Nb) normal modes, all the phonons observed in Figs. 1(a)–1(d), are unambiguously identified according to their frequency-shifting behavior, as listed in Table II.

The validity of the assignment of normal mode to each phonon is further supported by the variation of the FWHM with the concentration of Ta. Figure 2 shows the variation in phonon width as a function of Ta concentration ratio x. The

TABLE II. The assignment of Raman active modes of $Ba(Mg_{1/3}Nb_{2/3})O_3$ and $Ba(Mg_{1/3}Ta_{2/3})O_3$.

		BMN (cm^{-1})	BMT (cm^{-1})
2Ba(2*d*)	A_{1g}	105	106
	E_g	105	104
Ta (or Nb) (2*d*)	A_{1g}	296	264
	E_g	263	211
	A_{1g}	788	797
	A_{1g}	386	385
	E_g	437	432
6O(6*i*)	E_g	386	385
	E_g	175	158

oxygen-octahedron stretch mode, A_{1g}(O) 788~797 cm^{-1}, is the wider than all observed modes. The greater width is mostly due to the distortion of the oxygen octahedrons created by the short range of B-site 1:1 ordered structure.[19,24] The width of the A_{1g}(O) stretch mode increases from $x=0$ to 0.5 and then suddenly drops for the BMT sample. The decrease of the FWHM and the increase of the phonon frequency clearly indicate that BMT sample has a fairly good 1:2 ordered structure.[19–21]

The FWHM of 1:2 ordered modes, E_g(Ta/Nb) and A_{1g}(Ta/Nb), in Fig. 3 follow similar bell-like curves as x increases. The FWHMs of A_{1g}(Ta/Nb) and E_g(Ta/Nb) are small for the BMT ($x=1$) and BMN ($x=0$) ceramics, and the maximum width is exhibited by the most disturbed system, with $x=0.5$. These two phonon modes can be assigned because their phonon line shapes vary similarly with x. Clearly, A_{1g}(Ta/Nb) and E_g(Ta/Nb) are strongly related to the quality of 1:2 ordered structure, and the correlation of these modes with the microwave properties will be discussed shortly.

The width of the E_g(O) mode (437~432 cm^{-1}) linearly and gently decreases as the concentration of Ta increases, similar to the trend of the frequency shift shown in Fig. 1(c). However, the width of the A_{1g}(O)+E_g(O) (386 cm^{-1}) mode does not change with x. Like the A_{1g}(O)+E_g(O) phonon, the A_{1g}(Ba)+E_g(Ba) phonons near 105 cm^{-1}, with the smallest FWHM of all the observed phonons, is insensitive

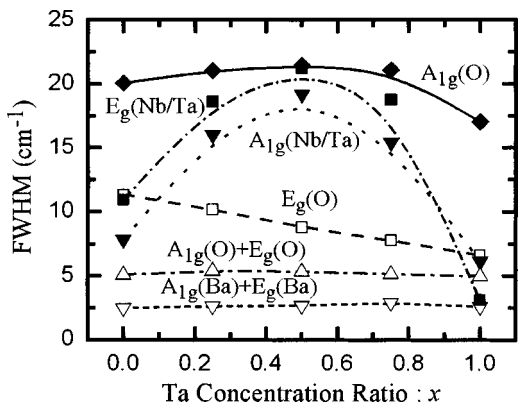

FIG. 2. The compositional variations of FWHMs of Raman phonons with x.

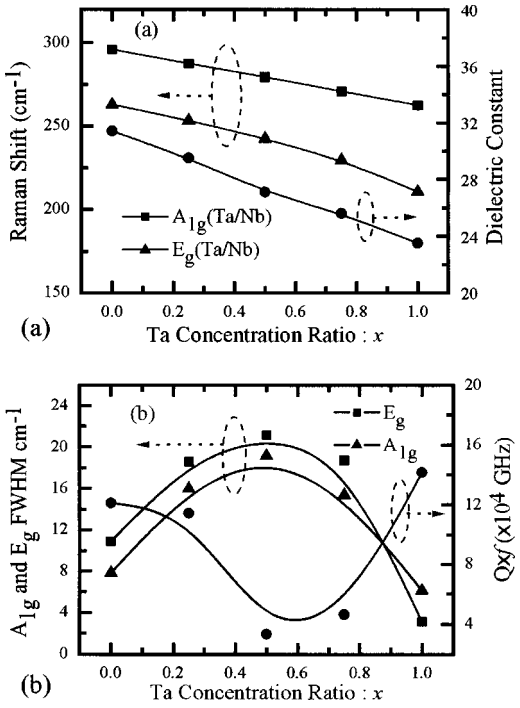

FIG. 3. Ta-concentration dependence of the characteristics of A_{1g}(Ta/Nb) and E_g(Ta/Nb) and the microwave properties of the xBMT–$(1-x)$BMN. (a) The Raman shift and the dielectric constant and (b) FWHM and the $Q\times f$ value are plotted with x.

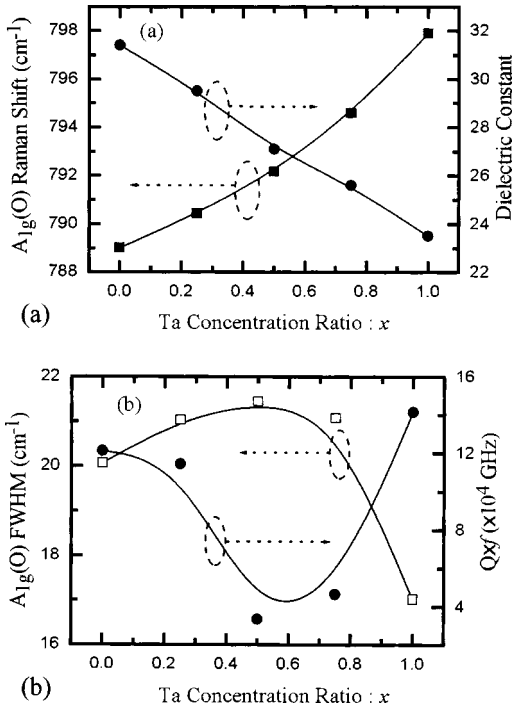

FIG. 4. Ta-concentration dependence of the characteristics of A_{1g}(O) phonon and the microwave properties for xBMT–$(1-x)$BMN materials. (a) The Raman shift and the dielectric constant and (b) FWHM and the $Q\times f$ value are plotted with x.

to Ta substitution. The consistency of the compositional dependence of FWHM with that of the frequency shift behavior exhibited by each normal mode supports the assignment of modes in Table II.

B. Correlation of microwave dielectric properties with phonon vibrations

Figures 3(a) and 3(b) present the variations of the dielectric constant K, and the quality factor, $Q\times f$, of the xBMT–$(1-x)$BMN with x, respectively. The Raman shifts and the linewidths of the A_{1g}(Ta/Nb) and E_g(Ta/Nb) 1:2 ordered modes are also plotted for comparison. Several studies[1–3,6,12,13] have demonstrated that a highly ordered 1:2 structure exhibits a higher $Q\times f$ value than the low-grade ones. Hence, as shown in Fig. 3, the 1:2 phonon modes are expected to correlate with the microwave properties of xBMT–$(1-x)$BMN. Figure 3(a) shows that the microwave dielectric constants and the Raman shifts of A_{1g}(Ta/Nb) and E_g(Ta/Nb) phonons vary linearly with the concentration of Ta. Figure 3(b) shows the $Q\times f$ values and 1:2 phonon widths against x. When the sample contains both Ta and Nb atoms, the degree of 1:2 ordering of its structure is degraded. Therefore, for $x=0.5$, the linewidths of the A_{1g}(Ta/Nb) and E_g(Ta/Nb) phonons to be broad, and the $Q\times f$ values to be low, as shown in Fig. 3(b).

Samples with a greater degree of 1:2 ordered structure are known to exhibit better microwave responses, which fact can explain the result shown in Fig. 3. However, the relationship between Ta/Nb atomic vibration and the microwave properties of perovskite ceramics is not easy to understand. In some cases, although $A(B'_{1/3}B''_{2/3})O_3$ ceramic samples were intended to be grown with 1:2 order, the intensities of the 1:2 ordered phonons were too low to analyze.[4,5,8,11,21] Therefore another indication of the quality of 1:2 ordered structure for $A(B'_{1/3}B''_{2/3})O_3$ ceramics is required.

Figure 4(a) shows that the oxygen-octahedron stretch mode around 788~797 cm^{-1} [A_{1g}(O)] shifts upward significantly with Ta concentration, while the K value decreases as x increases. The higher normal mode frequency of TaO_6 octahedral cages than that of NbO_6 cages indicates that the Ta–O bonds are stronger than the Nb–O bonds. This concludes that the smaller K value is due to the rigidity of the TaO_6 octahedral cages.

Figure 4(b) compares the compositional dependence of the FWHM of the A_{1g}(O) mode and that of $Q\times f$ value of xBMT–$(1-x)$BMN. Although the BMT material exhibits a markedly better dielectric loss (that is, a higher $Q\times f$ value than the BMN material), the $Q\times f$ values do not increase monotonically with the proportion of BMT in xBMT–$(1-x)$BMN ceramics. The large FWHM of A_{1g}(O) mode at $x=0.5$ indicates high dielectric loss (small $Q\times f$ value), when TaO_6, NbO_6, and MgO_6 octahedrons coexist in xBMT–$(1-x)$BMN. The smaller FWHMs at $x=1$ and 0 indicate that the coherency of the A_{1g}(O) stretch vibration is high. This result implies that the FWHMs of A_{1g}(O) stretch phonons in xBMT–$(1-x)$BMN exactly reflect the quality of the oxygen-octahedron structure, which is strongly correlated with the $Q\times f$ value. Figures 4(a) and 4(b) show that the nature of the oxygen-octahedron stretch phonon is strongly related to the microwave dielectric properties of xBMT–$(1-x)$BMN perovskite ceramics.

V. CONCLUSION

A Raman study of 1:2 ordered xBMT$-(1-x)$BMN compound was made, and Raman active phonons were completely assigned. The stretch mode of oxygen octahedron has the largest FHWM, and is the only blueshifted mode as Ta concentration increases. This finding implies that the oxygen octahedrons become rigid as Ta concentration increases. Oxygen octahedrons form a three-dimensional network in xBMT$-(1-x)$BMN ceramics; therefore, the stretch vibration of oxygen octahedron is strongly correlated with the microwave properties. Besides the 1:2 ordered structure, the rigidity of the oxygen octahedron caused by the substitution of a larger Ta atom for Nb atom is the primary reason for the reduced dielectric constant and the increased Q factors of BMT. This conclusion may also apply to similar $A(B'_xB''_y)O_3$ perovskite ceramic materials.

VI. ACKNOWLEDGMENT

The authors would like to thank the National Science Council, Republic of China, for financially supporting this research under Contract Nos. NSC 91-2112-M-003-024, NSC 91-2622-E-007-032, and NSC 92-2218-E-003-001.

[1] S. Nomura, K. Toyama, and K. Kaneta, Jpn. J. Appl. Phys., Part 2 **21**, L642 (1982).
[2] R. Guo, A. S. Shalla, and L. E. Cross, J. Appl. Phys. **75**, 4704 (1994).
[3] S. Nomura, T. Konoike, Y. Sakabe, and K. Wakino, J. Am. Ceram. Soc. **67**, 59 (1984).
[4] I. G. Siny, R. W. Tao, R. S. Katiyar, R. A. Guo, and A. S. Bhalla, J. Phys. Chem. Solids **59**, 181 (1998).
[5] R. L. Moreira, F. M. Matinaga, and A. Dias, Appl. Phys. Lett. **78**, 428 (2001).
[6] M. Iwata, H. Hoshino, H. Orihara, H. Ohwa, N. Yasuda, and Y. Ishibashi, Jpn. J. Appl. Phys. **39**, 5961 (2000).
[7] H. Ohwa, M. Iwata, H. Orihara, N. Yasuda, and Y. Ishibashi, J. Phys. Soc. Jpn. **70**, 3149 (2001).
[8] H. Idink and W. B. White, J. Appl. Phys. **76**, 1789 (1994).
[9] B.-K. Kim, H. Hamaguchi, I.-T. Kim, and K. S. Hong, J. Am. Ceram. Soc. **78**, 3117 (1995).
[10] S. Kawashima, M. Nishida, I. Ueda, and H. Ouchi, J. Am. Ceram. Soc. **66**, 421 (1981).
[11] A. Dias, V. S. T. Ciminelli, F. M. Matinagaa, and R. L. Moreira, J. Eur. Ceram. Soc. **21**, 2739 (2001).
[12] M. Sugiyama and T. Nagai, Jpn. J. Appl. Phys., Part 1 **32**, 4360 (1993).
[13] I. N. Lin, C. T. Chia, H. L. Liu, H. F. Cheng, and C. C. Chi, Jpn. J. Appl. Phys., Part 1 **41**, 6952 (2002).
[14] D. Kajfez and P. Guillon, *Dielectric Resonators* (Artech House, Norwood, MA, 1986), chap. 6.
[15] J. Krupka, K. Derzakowski, A. Abramowicz, M. E. Tobar, and R. G. Geyer, IEEE Trans. Microwave Theory Tech. **47**, 752 (1999).
[16] F. S. Galasso, *Structure, Properties and Preparation of Perovskite-Type Compounds*, 1st ed. (Pergamon, Oxford, 1969), pp. 13–15, 55.
[17] H. Tamura, D. A. Sagala, and K. Wakino, Jpn. J. Appl. Phys., Part 1 **25**, 787 (1986).
[18] Y. C. Chen, H. F. Cheng, H. L. Liu, C. T. Chia, and I. N. Lin, J. Appl. Phys. **94**, 3365 (2003).
[19] I. G. Siny, R. S. Katiyar, and A. S. Bhalla, J. Raman Spectrosc. **29**, 385 (1998).
[20] R. Ratheesh, M. Wohlecke, B. Berge, Th. Wahlbrink, H. Haeuseier, E. Ruhl, R. Blachnik, P. Balan, N. Santha, and M. T. Sebastian, J. Appl. Phys. **88**, 2813 (2000).
[21] F. Jiang, S. Kojima, C. Zhao, and C. Feng, Appl. Phys. Lett. **79**, 3938 (2001).
[22] T. Nagai, M. Sugiyama, M. Sando, and K. Nhhara, Jpn. J. Appl. Phys. **36**, 1146 (1997).
[23] M.-L. Hu, C.-T. Chia, J. Y. Chang, W.-S. Tse, and J.-T. Yu, Mater. Chem. Phys. **78**, 358 (2003).
[24] J. D. Freire and R. S. Katiyar, Phys. Rev. B **37**, 2074 (1988).